HHS Public Access

Author manuscript

FEBS J. Author manuscript; available in PMC 2022 January 01.

Published in final edited form as:

FEBS J. 2021 January ; 288(1): 142–159. doi:10.1111/febs.15449.

Neuropathy-associated histidyl-tRNA synthetase variants attenuate protein synthesis in vitro and disrupt axon outgrowth in developing zebrafish

Patrick Mullen[1], **Jamie A. Abbott**[1], **Theresa Wellman**[2], **Mahafuza Aktar**[1], **Christian Fjeld**[1], **Borries Demeler**[3], **Alicia M. Ebert**[4], **Christopher S. Francklyn**[1]

[1]Department of Biochemistry, University of Vermont

[2]Department of Pharmacology, University of Vermont

[3]Department of Chemistry & Biochemistry, University of Lethbridge

[4]Department of Biology, University of Vermont

Abstract

Charcot-Marie-Tooth disease (CMT) encompasses a set of genetically and clinically heterogeneous neuropathies characterized by length dependent dysfunction of the peripheral nervous system. Mutations in over 80 diverse genes are associated with CMT, and aminoacyl-tRNA synthetases (ARS) constitute a large gene family implicated in the disease. Despite considerable efforts to elucidate the mechanistic link between ARS mutations and the CMT phenotype, the molecular basis of the pathology is unknown. In this work, we investigated the impact of three CMT-associated substitutions (V155G, Y330C, R137Q) in the cytoplasmic histidyl-tRNA synthetase (HARS1) on neurite outgrowth and peripheral nervous system development. The model systems for this work included a nerve growth factor stimulated neurite outgrowth model in rat pheochromocytoma cells (PC12), and a zebrafish line with GFP/RFP reporters of sensory and motor neuron development. Expression of CMT-HARS1 mutations led to attenuation of protein synthesis and increased phosphorylation of eIF2α in PC12 cells and was accompanied by impaired neurite and axon outgrowth in both models. Notably, these effects were phenocopied by histidinol, a histidyl-tRNA synthetase inhibitor, and cycloheximide, a protein synthesis inhibitor. The mutant proteins also formed heterodimers with wild-type HARS1, raising the possibility that CMT-HARS1 mutations cause disease through a dominant negative mechanism. Overall, these findings support the hypothesis that CMT-*HARS1* alleles exert their toxic effect in a neuronal context, and lead to dysregulated protein synthesis. These studies

To whom correspondence should be addressed: Christopher Francklyn, Larner College of Medicine, Health Sciences Complex, 89 Beaumont Ave., Burlington, VT 05405, Christopher.Francklyn@med.uvm.edu, Alicia Ebert, Department of Biology, 109 Carrigan Dr, 120A Marsh Life Science, Burlington, VT 05405, amebert@uvm.edu.

AUTHOR CONTRIBUTIONS

P.M. planned experiments, performed experiments, analyzed data, wrote the paper. J.A. planned experiments, performed experiments. T.W. supervised experiments, performed experiments. M.A. performed experiments, analyzed data. C.F. performed experiments, analyzed data. B.D. performed experiments, analyzed data. A.E. planned experiments, supervised experiments, wrote the paper. C.F. planned experiments, supervised experiments, wrote the paper.

CONFLICTS OF INTEREST:

The authors declare no competing interests.

demonstrate the value of zebrafish as a model for studying mutant alleles associated with CMT, and for characterizing the processes that lead to peripheral nervous system dysfunction.

Abstract

Peripheral neuropathy associated histidyl-tRNA synthetase (HARS) variants form heterodimers with wild-type HARS and disrupt peripheral nervous system structure and function. Defects in neurite outgrowth are linked to attenuation of protein synthesis and induction of eIF2α phosphorylation. The cellular effects of mutant HARS were phenocopied by inhibition of HARS activity (histidinol) or protein synthesis (cycloheximide). These results suggest that HARS inhibition and dysregulated protein synthesis may be key pathogenic processes in peripheral neuropathy.

Graphical Abstract

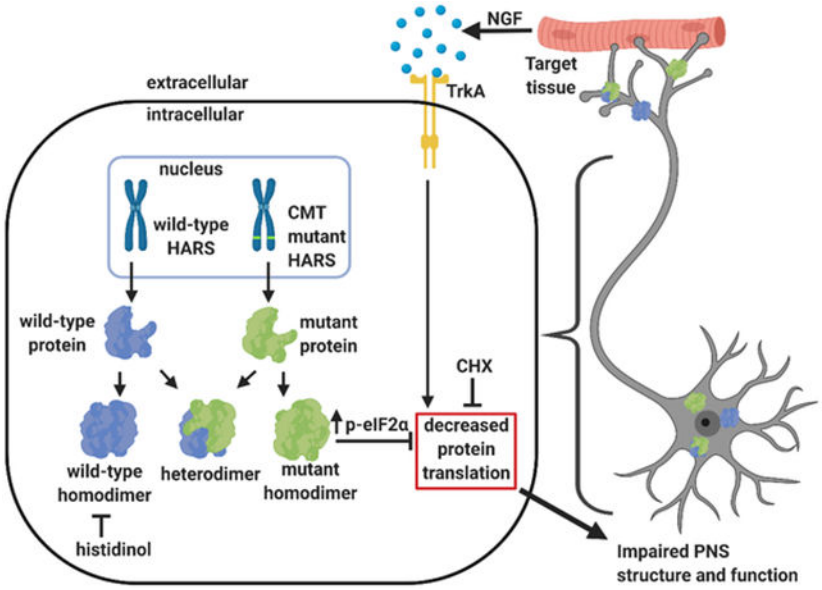

Keywords

Charcot-Marie-Tooth disease; peripheral neuropathy; aminoacyl-tRNA synthetase; protein synthesis; tRNA

INTRODUCTION

Charcot-Marie-Tooth disease (CMT) is a clinically and genetically heterogenous collection of inherited peripheral neuropathies with a worldwide prevalence of 1 in 3,300 [1]. CMT is commonly characterized by length-dependent dysfunction of the sensory and motor components of the peripheral nervous system (PNS), often resulting in muscle weakness and atrophy in the distal extremities as well as sensory disturbances such as hypoesthesia and neuropathic pain [2]. CMT is divided into two principle subtypes, demyelinating (CMT1) and axonal (CMT2), which differ with respect to clinical electrophysiology and nerve biopsy

findings [3]. Clinically, CMT1 patients exhibit sharply reduced nerve conduction velocities arising from myelination defects, while CMT2 patients typically present with axonal degeneration. Some 80 different genes have been linked to CMT via mutations that have been demonstrated to be pathogenic [4]. While CMT1 genes are commonly related to Schwann cell biology [5], genes that are linked to CMT2 span a wide range of functions, including axonal transport, mitochondrial dynamics and turnover, vesicular transport, and protein homeostasis [6, 7].

Aminoacyl-tRNA synthetases (ARS) represent a particularly large gene family linked to the disease [8, 9]. ARS catalyze the attachment of amino acids to their cognate tRNAs in an early reaction of protein synthesis that is universal in all kingdoms of life [10]. The human nuclear genome encodes 37 ARS enzymes, including 18 cytoplasmic, 17 mitochondrial, and 2 dual compartment enzymes [8, 11]. While ARS are best known for their role in protein synthesis, non-canonical functions that have been reported include the regulation of transcription [12], translation [13], angiogenesis [14], and immunity [15]. Owing to the essential nature of the aminoacylation reaction in translation, the association of mutations in ARS genes with a broad spectrum of human diseases is unsurprising [8]. Nevertheless, ARS mutations often preferentially affect the nervous system, which has not been explained [11, 16]. While ARS mutations exhibit a variety of inheritance patterns and can influence the nervous system in different ways, the autosomal dominantly inherited CMT mutations have received considerable research attention [8, 9]. Thus far, mutations in the cytoplasmic glycyl- (GARS1) [17–19], tyrosyl- (YARS1) [20, 21], alanyl- (AARS1) [22–25], histidyl- (HARS1) [26–28], and tryptophanyl- tRNA synthetases (WARS1) [29] have all been convincingly linked to CMT. Notably, all ARS genes associated with CMT encode enzymes that function as dimers.

The association of CMT with multiple structurally diverse ARS raises the question of whether a pathogenic mechanism common to multiple enzymes may be involved [8, 9]. Currently, the extent to which pathogenesis involves loss of ARS canonical function in protein synthesis, versus other potential functions, is unresolved [8, 9, 17, 30]. While most mutant alleles confer loss-of-function effects, some ARS variants that appear to retain significant levels of aminoacylation function are nevertheless associated with CMT [20, 25, 31]. In addition to impairing aminoacylation [18, 20, 23, 25, 28, 29, 32], ARS mutations linked to CMT have been reported to affect dimerization [33, 34] and localization properties [20, 32, 34, 35]. Those CMT-ARS variants that have been overexpressed in the *Drosophila* model have been shown to impair global cellular translation in neurons, including variants (GARS1 E71G & YARS1 E196K) that retain at least partial aminoacylation function [36]. These observation have led to proposals that inhibition of protein synthesis may be a common effect of CMT-ARS mutations [17, 20, 29, 32, 36].

An additional outstanding question is the specific nature of the insult to the peripheral nervous system caused by these mutant alleles. For example, the relative involvement of developmental defects, axonal degeneration, and neuronal apoptosis is unknown. CMT-ARS expression has been shown to alter neuronal morphology, but death of neurons has not been observed in a mouse model of CMT [37]. Despite the variable onset and apparent age-

dependent axonal degeneration seen in many CMT patients, several animal models suggest that CMT-ARS mutants disrupt neuronal morphology during development [25–27, 38–40].

At present, the potential connection between decreases in aminoacylation function and the more complex phenotypes of peripheral nervous system diseases like CMT is unclear. In this study, we investigated this question through the analysis of HARS1 variants genetically linked to CMT [27, 28]. Eight different *HARS1* alleles have been described, and those characterized *in vitro* behave as loss-of-function mutations [26–28, 41]. Here, we investigated three different CMT-HARS1 substitutions (V155G, Y330C, R137Q) proximal to the HARS1 active site [26, 28] for their impact on neuronal development. Differentiated PC12 cells expressing these mutants displayed diminished length of the longest neurite, decreased protein synthesis, and increased phosphorylation of eIF2α, a marker of the integrated stress response (ISR) [42]. The neurite shortening and protein synthesis defects were phenocopied by administration of the amino alcohol histidinol or subtoxic doses of cycloheximide. When injected into zebrafish embryos, the CMT-HARS1 mutants produced axonal defects and compromised swimming behavior, as indicated in a touch response assay. None of the mutants affected HARS1 localization, and all mutants readily formed heterodimers with wild-type HARS1. The implications of these results for our understanding of ARS-related CMT are discussed in light of current models.

RESULTS

Expression of CMT-HARS1 mutants disrupts neurite outgrowth in differentiated PC12 cells

Previous work in both cellular and animal models indicates that CMT-ARS alleles impair axon structure during development, leading to guidance defects and reduced formation of neuromuscular junctions. In particular, mutations in GARS1 [38, 39], YARS1 [36], HARS1 [26, 27] and AARS1 [25] have been observed to disrupt axonal structure during development, whereas WARS1 and AARS1 mutations associated with CMT have been reported to impair neurite outgrowth *in vitro* [29, 43]. To investigate the impact of CMT-HARS1 expression on cellular structure, we employed a nerve growth factor (NGF) induced neurite outgrowth assay in the immortalized rat pheochromocytoma line, PC12. This cell line represents a well-established model for studying neurite outgrowth and NGF signaling, as well as disease associated mutations that disrupt these processes [44, 45]. Among the HARS1 mutants in our collection, we focused first on the V155G and Y330C variants (Fig. 1A) as they are genetically linked to CMT, substitute conserved active site residues (Fig. S1), and have been characterized in detail biochemically [28].

To determine the effect of CMT-HARS1 mutants on neurite outgrowth, cells were transfected with plasmids encoding GFP tagged wild-type or mutant HARS1 and then treated with NGF, causing cells to assume a neuron-like morphology (Fig. 1B) and upregulate the growth cone protein GAP-43 (Fig. 1C). Western blot and immunofluorescence imaging analysis of GFP indicated that GFP-tagged mutant and wild-type proteins accumulate to comparable levels (Fig. 1D,E), consistent with previous reports that the mutations are not destabilizing [28]. In a comparison of PC12 cells transfected with either wild-type or mutant HARS1, the size of the cell body and the number of neurites was unchanged (Fig. 1D,F,G). By contrast, the length of the longest neurite process was

significantly decreased in the CMT mutant transfected cells, relative to wild-type (Fig. 1D,H). To further validate this result, PC12 cells were transfected with the R137Q CMT-HARS1 variant, and then allowed to differentiate. Previously, this mutant has been shown cause abnormal axon guidance and neurotoxicity during development in *C. elegans* [46]. Consistent with these earlier reports, R137Q HARS1 expression induced shortening of the longest neurite process (Fig. 1H), but left other parameters unaffected (Fig. 1F,G). As a final control to assess the impact of these mutants on cell viability, cells were stained for cleaved caspase-3 and imaged (data not shown). Based on the absence of a signal, none of the mutants appeared to promote apoptosis. In summary, the results of these experiments suggest that the principal phenotypic consequence of overexpression of CMT-HARS1 mutants in the context of differentiating PC12 cells is shortening of the longest neurite.

In view of the conflicting models proposed to account for CMT-ARS pathophysiology, and the uncertain contribution of losses in aminoacylation function to pathology, we investigated whether neurite shortening could be induced by attenuating HARS1 aminoacylation function via a mechanism independent of CMT mutations *per se*. These experiments employed the amino alcohol histidinol, which binds to the histidine binding site in HARS1 but prevents the formation of histidyl adenylate [47]. *In vitro*, histidinol leads to the reversible arrest of protein synthesis by several different mechanisms, including decreasing the initiation of protein synthesis [48] and promoting ribosome stalling [49]. In contrast to the transfection process used to introduce CMT-HARS1 mutants, which only modifies a fraction of cells in the population (approximately 10%), histidinol treatment affects all cells in the culture. Histidinol treatment had a dose dependent effect on PC12 cells, such that cells receiving 0.5 mM histidinol displayed normal neurite outgrowth, while cells treated with 1 mM and 2 mM histidinol exhibited significant decreases in average length of the longest neurite (Fig. 1I,J). In addition, decreased neurite outgrowth mediated by histidinol treatment was associated with reduced levels of GAP-43, which is normally upregulated in PC12 cells following NGF treatment [44] (Fig. 1K,L). Consistent with previous studies [50], viability was unaffected at the doses of histidinol tested (one-way ANOVA, $p = 0.3497$). In summary, decreases in HARS1 aminoacylation function linked to either CMT mutations or the competitive inhibitor histidinol produced similar impacts on NGF induced neurite outgrowth in PC12 cells.

Neurite shortening caused by CMT-HARS1 variants is linked to attenuated protein synthesis and induction of eIF2α phosphorylation

Previous biochemical characterization of the HARS1 mutants investigated above demonstrate that each is associated with a significant decrease in aminoacylation function [28, 46]. However, questions remain regarding the potential impact of these catalytic defects on protein synthesis in various cell types. For example, characterization of fibroblasts from a CMT patient carrying a V133F *HARS1* allele showed that despite a reduction in enzyme activity, there was no detectable effect on protein synthesis [41]. To determine if the effect of CMT-*HARS1* alleles on protein synthesis is cell type specific, we analyzed protein synthesis in differentiated PC12 cells expressing CMT-HARS1. Previously, several GARS1 and YARS1 mutations associated with CMT were shown to reduce protein synthesis in *Drosophila* sensory and motor neurons [36]. We quantified protein synthesis in transfected

and differentiated PC12 cells by use of the puromycin analog, OP-puromycin, which is incorporated into nascent polypeptides and can be detected by use of a florescent probe. Transfection with each of the CMT-HARS1 variants led to reductions in OP-puromycin incorporation on the order of 20–30% relative to wild-type and untransfected cells, representing a significant impact on protein synthesis (Fig. 2A,B). Consistent with the previous neurite outgrowth results, treatment with 1 mM histidinol produced a decrease in protein synthesis similar to overexpression of the CMT-*HARS1* alleles (Fig. 2A,B). To further validate the link between decreased protein synthesis and diminished neurite outgrowth, we also tested the effects of a low dose of the protein synthesis inhibitor, cycloheximide (CHX). At a concentration of 45 nM, CHX treatment reduced neurite length in differentiated PC12 cells (Fig. 2C,D) but did not affect cell viability as indicated by trypan blue staining (Fig. 2E).

Owing to the reduction in catalytic function associated with CMT-HARS1 variants, their overexpression might promote accumulation of uncharged tRNA leading to induction of integrated stress response pathways triggered by phosphorylation of eIF2α. To test this hypothesis, PC12 cells were transfected with CMT-HARS1, differentiated with NGF, and stained for phosphorylated eIF2α. Fluorescence intensity corresponding to p-eIF2α was increased 2 to 2.5-fold in cells transfected with mutant HARS1 compared to the wild-type control (Fig. 2F,G). To determine whether these effects are the result of reduced aminoacylation as opposed to other ARS functions, western blotting was used to assess the extent of eIF2α phosphorylation in differentiated PC12 cells treated with 1–2 mM histidinol. These experiments confirmed the results of immunofluorescence experiments, and showed that inhibition of HARS1 by a small molecule similarly induced eIF2α phosphorylation (Fig. 2H,I). Thus, the neurite outgrowth defects described earlier are likely to be the result of decreased protein synthesis, which appears to be linked to induction of the ISR.

CMT-HARS1 variants localize normally in PC12 and MN1 cells

The link between neurite outgrowth defects and the induction of translational stress seen in PC12 cells versus fibroblasts supports the hypothesis that a neuronal context is critical for understanding the consequences of CMT-ARS mutants. Previously, abnormal cellular localization of mutant ARS proteins has been invoked to explain the neuron specific phenotype observed in CMT patients [20, 32, 34], but the localization of CMT-HARS1 mutants has not been assessed in prior reports [27, 28]. When GFP-tagged constructs encoding either wild-type or mutant HARS1 were overexpressed in differentiated PC12 cells, GFP staining corresponding to HARS1 was observed diffusely throughout the cytoplasm and neurites, with a slight perinuclear enrichment (Fig. 3A, top row). Moreover, the ratio of HARS1 intensity in the neurites versus soma was similar between wild-type transfected, mutant transfected, and untransfected cells (Fig. 3B). Due to the fact that the longest neurites were shorter in mutant transfected cells (Fig. 1F), we correlated neurite staining intensity to neurite length to ensure that the localization did not appear to be unaffected due to fewer long neurites in mutant transfected cells. We found no correlation between neurite staining intensity and neurite length (Fig. 3C), indicating that HARS1 localization in distal neurites is not affected by neurite length. As an additional confirmation of these results, we investigated the localization of HARS1 protein in the MN1 cholinergic

motor neuron cell line, and found that endogenous, wild-type, and mutant HARS1 all localize diffusely throughout the cytoplasm (Fig. 3A, bottom row), unlike wild-type GARS1 [32]. Together, these data suggest that protein localization is not affected by CMT-HARS1 mutations, indicating that any difference in this property is unlikely to explain the impact on neurite physiology.

Expression of Y330C and V155G-HARS1 impairs structure and function of motor and sensory neurons in developing zebrafish

While PC12 cells represent a tractable and high-throughput model for assessing neurite outgrowth, they lack many features of neurons including dendrites, axons, and other physiological characteristics. Moreover, critical aspects of neuronal physiology provided by the context of neighboring cell types are lacking in *in vitro* systems. To address these limitations, we sought an animal model where neuronal structure and function could be followed over time in a developmental context. Accordingly, we employed a transgenic zebrafish line in which sensory and motor divisions of the PNS are selectively visualized via expression of fluorescent reporter proteins under the control of sensory (ngn1:GFP) and motor neuron (mnx1:RFP) specific promoters [51, 52]. Consistent with observations *in vitro*, the overexpression of human CMT-HARS1 mutants disrupted axonal morphology of dorsal root ganglion cells (DRG) (Fig. 4A-C). Specifically, axons were shorter (Fig. 4D) and had misguided ventral projections (Fig. 4E) in fish injected with Y330C and V155G HARS1 mRNA. Additionally, the ventrally projecting CaP motor axons were shorter in CMT-HARS1 overexpressing embryos than controls (Fig. 4A’-C’,F). The observed changes in axon length were not a result of decreased body size, as the overall body length of wild-type and CMT-HARS1 injected fish was similar (Fig. 4G).

To investigate the functional consequences of abnormal PNS morphology observed in CMT-HARS1 expressing zebrafish, we performed touch evoked escape assays in which fish are stimulated with forceps and swimming behavior is monitored. Due to the PNS mispatterning observed, it is unsurprising that CMT-HARS1 injected fish did not respond consistently to mechanical stimuli. Not only did the Y330C and V155G expressing fish respond less frequently to touch stimuli (Fig. 4H), but the percentage of normal swimming responses was also decreased, and often resembled a twitch rather than a coordinated swimming response (Fig. 4I).

We hypothesized that the effect of the CMT-HARS1 mutations on axon outgrowth and guidance in zebrafish might be a consequence of the impact of these mutants on protein synthesis [36]. To test this hypothesis, zebrafish embryos were treated with sub-toxic concentrations of cycloheximide (CHX) (Fig. 4G,H). Previous studies reported that 10 μM CHX disrupts neuromuscular junction morphology and decreases body size in zebrafish [35]. When zebrafish embryos were treated with 2.5 μM CHX at 24 hours post-fertilization (hpf), we observed a striking reduction in DRG axon length at 48 hpf (Fig. 4L), while body length and survival were unaffected (Fig. 4 M,N). Together, these results indicate that subtoxic doses of CHX disrupts neurite morphology, further suggesting that neurons are particularly sensitive to protein synthesis inhibition during the process of neurite outgrowth. The effects on neurite outgrowth observed in PC12 cells were faithfully recapitulated in a

zebrafish model of neuronal development, where environmental cues that regulate axon guidance from various cell types are present.

CMT-HARS1 variants dimerize with wild-type HARS1

One hypothesis to account for the toxic gain-of-function associated with CMT-ARS alleles is that the mutant proteins interfere with wild-type ARS function via a dominant negative mechanism [17, 53]. Since all of the ARS-CMT alleles are associated with dimeric enzymes, we considered the hypothesis that mutant HARS1 interferes with wild-type function by forming heterodimers with wild-type subunits, compromising their protein synthesis function. In line with this hypothesis, we previously reported that the V155G and Y330C mutant proteins exhibit sedimentation behavior identical to the wild-type protein, consistent with formation of stable homodimers [28]. Because the R137Q substitution alters a highly conserved dimer stabilizing interaction at the dimer interface, we used analytical ultracentrifugation to test the possibility that this variant cannot form stable dimers. Surprisingly, the sedimentation velocity of R137Q was similar to that of wild-type (Fig. 5A), indicating that R137Q forms a stable homodimer. To investigate the possibility that one or more of the HARS1 mutants are able to dimerize with wild-type HARS1, HEK-293 cells were co-transfected with FLAG-tagged wild-type HARS1 and either wild-type or mutant (V155G, Y330C, R137Q) GFP-tagged HARS1. Extracts from these cells were immunoprecipitated with an anti-FLAG antibody, and then probed for the presence of GFP-conjugated subunits. Consistent with our hypothesis, wild-type and mutant HARS1 were both immunoprecipitated by wild-type HARS1, providing evidence that the substitutions characteristic of CMT-mutant HARS1 variants do not reduce the ability to dimerize with wild-type HARS1 (Fig. 5B). Additionally, when the same experiment was performed with GFP-tagged human HARS1 and FLAG-tagged zebrafish hars, human HARS1 was observed to immunoprecipitate zebrafish hars (Fig. 5C).

DISCUSSION

In this study, we demonstrate that overexpression of a subset of HARS1 mutants linked to CMT causes neurite shortening and defects in axonal guidance in differentiated PC12 cells and zebrafish, respectively. The mutant proteins accumulated to wild-type levels, reduced global protein synthesis, and induced phosphorylation of eIF2α, a marker of the ISR. Moreover, the effects of the mutants on neurite shortening were phenocopied by the specific HARS1 inhibitor (histidinol) and the protein synthesis inhibitor cycloheximide. At the organismal level, overexpression of CMT mutants in developing zebrafish caused abnormalities in touch response and swimming behavior. Finally, CMT-HARS1 mutants localized normally and were observed to readily form dimers with wild-type HARS1.

Neurological diseases caused by mutations in cytoplasmic ARS genes can be divided into two broad groups, dominantly inherited peripheral neuropathies and recessively inherited developmental encephalopathies [8, 11, 16]. The recessive genotypes typically cause drastic reductions in ARS levels and/or activity [54–57], leading to the general consensus that this group of diseases is associated with loss of aminoacylation function [8, 58]. By contrast, the relationship between aminoacylation and the dominantly inherited peripheral neuropathies is

less clear. In the case of HARS1, the correlation between loss of aminoacylation and pathogenicity is suggested by the uniform localization of CMT mutations in close proximity to the active site, the strong reductions (100–1000 fold) in catalytic activity, and inability of mutant alleles to complement a haploid yeast *hts1* deletion strain. In contrast, the link between loss of aminoacylation and pathogenicity is less clear for GARS1 and YARS1 variants. GARS1 mutations are not uniformly located near the active site, and select *GARS1* and *YARS1* alleles appear to retain aminoacylation activity [20, 31, 34]. Additionally, it has been argued in both systems that pathogenicity is at least partially due to the ability of the mutant proteins to engage in ectopic interactions with proteins outside of the translation apparatus [40, 59–64]. For HARS1, recent work suggests that the enzyme may act as an immunomodulator in the extracellular context [65], but there is as yet no reported evidence linking this activity to PNS pathology, and no evidence of ectopic interactions for the mutant enzymes. The contribution of putative secondary ARS functions to CMT pathology was not tested explicitly in our study, but other recent results bear on this question [66].

Cellular context has emerged as a critical factor that may influence the relationship between loss of aminoacylation and CMT pathology. As noted above, decreases in the ability of CMT-ARS alleles to complement the corresponding yeast knockout strain have been employed to identify putative loss-of-function mutations [8, 67]. While such experiments can provide a valuable initial view of a given allele's ability to support eukaryotic protein synthesis, determining the consequences of expressing that same allele in different cell types in a multicellular organism can be particularly illuminating. For example, the E71G-GARS1 mutation shown to complement a *grs1* deletion in yeast was unable to complement *gars* deletion in *Drosophila* olfactory neurons [68]. For the CMT-HARS1 variants, weak complementation in yeast was only observed for a single allele (V155G), and all mutants led to decreased protein synthesis in NGF stimulated PC12 cells (Fig. 2B). In the context of mammalian cells, cell type specific impacts on protein synthesis were seen for the CMT-HARS1 mutants. Overexpression of CMT-*HARS1* alleles and administration of subtoxic doses of histidinol to NGF differentiated PC12 cells both led to essentially equivalent decreases in protein synthesis. In contrast, protein synthesis levels in dermal fibroblasts derived from a peripheral neuropathy patient with a *HARS1* allele that substitutes an active site residue were unchanged relative to those of control fibroblasts, despite a ~25% decrease in aminoacylation activity [41]. The decreases in protein synthesis in NGF stimulated PC12 cells observed in our study are consistent with the hypothesis that cell types with specialized protein synthesis requirements, such as neurons, may be particularly sensitive to the reduced function of CMT-ARS mutants [17, 69]. Notably, all CMT-ARS variants that have been studied in the *Drosophila* model have been shown to impair global cellular translation in neurons [36].

Models in which ARS-CMT pathology is linked to protein synthesis provide a rationale for the observation that many CMT associated mutations exhibit impacts on primary function but fail to account for the dominant nature of these alleles. Defects in aminoacylation and protein synthesis *in vivo* could result from haploinsufficiency or a dominant negative mechanism. Haploinsufficiency is unlikely to account for ARS-CMT pathology because heterozygous GARS1 knockout mice do not develop peripheral neuropathy [37], null ARS alleles have been identified in healthy individuals [69, 70], and heterozygous parents of

children with neurodevelopmental disorders caused by biallelic ARS mutations are phenotypically normal [55, 57]. In support of a dominant negative explanation, all ARS with definitive genetic linkage to CMT (GARS1, YARS1, AARS1, HARS1, and WARS1) function as dimers, indicating that interference with wild-type protein may be essential for pathology.

These observations suggest that a dominant negative mechanism may account for ARS-CMT pathology [53, 69]. Among the criteria for a dominant negative effect are that (a) the protein typically functions as a dimer; (b) the mutated allele produces a protein that is expressed and is stable; (c) the mutated protein has reduced function; (d) the mutation(s) do not block the ability of the protein to form heterodimers with wild type; (e) the resulting wild type-mutant heterodimer has reduced function [53]. The data reported here and in prior studies suggest that in the case of HARS1 associated CMT, these criteria are fulfilled. Notably, we found that all CMT-HARS1 mutants tested were able to form heterodimers with wild-type HARS1 (Fig. 5). Heterodimers were also formed between human and fish enzymes, which would be necessary for dominant negative effects when the human alleles are introduced into zebrafish. Other CMT-ARS mutants also fulfill many of the requirements for a dominant negative mechanism. Multiple GARS1 and YARS1 mutants have been shown to form heterodimers with wild-type protein [20, 34], and YARS1 and WARS1 mutations have dominant negative effects on aminoacylation in yeast and mammalian cells, respectively [20, 29]. Finally, *in vivo* experiments suggest that the G526R GARS1 mutation impairs neuromuscular junction morphology through a dominant negative mechanism [35].

The experiments reported here do not specifically address the functionality of a CMT-HARS1-wild-type heterodimer, one of the criteria for the dominant negative mechanism [53]. However, the fact that HARS1 inhibition by histidinol phenocopied the effects of CMT-HARS1 mutations suggests that results in mutant transfected cells are related to impaired aminoacylation. In previous work we investigated the activity of a mutant (R259H)-wild-type heterodimer of *E. coli* HisRS [71]. This heterodimer synthesizes histidyl-adenylate at precisely half the stoichiometry of the wild-type enzyme [71]. Owing to the close proximity of CMT-HARS1 mutant substitutions to the corresponding catalytic arginine (R326) in the human HARS1 enzyme, wild-type-CMT-HARS1 heterodimers are expected to behave in a fashion similar to wild-type-R259H heterodimers with respect to kinetics. Based on our model of alternating active site catalysis [72], the significantly reduced catalytic function of the mutant monomer is expected to prevent aminoacylated tRNA release by the heterodimer, a prediction readily testable by single turnover kinetics. Defects in product release resulting from heterodimer formation would be expected to cause a depletion of the histidyl-tRNA pool *in vivo*, with important downstream consequences.

A key finding of this study is that CMT-HARS1 overexpression and subtoxic treatments with histidinol and cycloheximide all produced similar effects with respect to reduced protein synthesis and inhibition of neurite outgrowth. The integrated stress response was induced by both CMT-HARS1 mutants and histidinol (Fig. 2). Notably, CMT-HARS1 mutants and histidinol treatment both block aminoacylation at the adenylation step, likely producing the stalled complexes previously described [28, 47]. Histidinol is a known reversible inhibitor of protein synthesis [73], and has recently been shown to promote

ribosome stalling and induction of the ISR, likely via activation of GCN2 [49, 74]. Recent reports suggest that the P-stalk of stalled ribosomes potently binds and activates GCN2, thereby inducing the ISR [75]. In contrast, cycloheximide acts downstream of aminoacylation by binding to the ribosome E-site and blocking translocation, thereby promoting stalling of ribosomes [76]. Our observation that CMT-HARS1 mutant overexpression, histidinol, and cycloheximide treatment all produced similar impacts on protein synthesis and neurite extension while leaving viability unaffected highlights altered proteostasis and the ISR as key processes that are likely linked to CMT pathology. Other strong connections between perturbations in the ISR and neurological diseases have been reported [42], but are by no means fully understood. Clearly, this connection merits more detailed study.

Prior to this work, in depth characterization of CMT-ARS alleles *in vivo* has been performed in *Drosophila,* mouse, and *C. elegans* models. Use of zebrafish as a CMT model has been limited, but is increasing. Use of *Drosophila* benefits from highly developed genetics and the ability to interrogate mutant ARS function in a cell type specific fashion [36, 77]. Yet, the invertebrate nature and differences between and fly and human nervous systems is a limitation. While currently limited to GARS1 mutations, mouse models of ARS-CMT have been very useful in highlighting the abnormalities that lead to altered neuronal structure and function [78], and have also identified potential therapeutic strategies [64, 66]. Nevertheless, early neurodevelopmental events are not readily accessible in the mouse, and there is substantial time and cost associated with the production of mouse lines with individual mutations. While relatively few studies have made use of *C. elegans*, it remains an excellent system for following neuronal patterning during development, and assessing neurotoxic effects [46].

The work described here provides validation for use of PC12 cells and zebrafish as cellular and animal models for ARS-CMT, respectively. Although PC12 cells are a useful tool for overexpression studies, they are limited by their neoplastic origin and the lack of true dendrites and axons. Furthermore, protein overexpression in cells and zebrafish does not precisely model the genotypes that cause dominant peripheral neuropathies. While this limitation could be addressed using patient cells or CRISPR knock-in approaches, knock-in of mutant HARS1 mutations is made challenging by the fact that the zebrafish *hars* gene encodes both cytoplasmic and mitochondrial enzymes [79]. Our data highlight the fact that zebrafish are an ideal intermediate between mice and lower animals in that they develop rapidly and are genetically tractable but possess the benefit of having a spinal cord and PNS that is structurally analogous to humans [80]. Consistent with those strengths, knockdown of AARS1 and microinjection of mRNA encoding three different CMT-AARS1 mutants was shown to disrupt PNS structure in zebrafish, although the specific neuronal consequences were not investigated [25]. In this work, we found that deficiencies in neurite outgrowth in zebrafish paralleled those seen in PC12 cells and were directly linked to abnormal swimming behavior. The latter defects were highly reminiscent of those seen with the choline acetyltransferase mutant *Bajan*, which is associated with impaired synaptic transmission and motor function [81]. Going forward it will be essential to test whether zebrafish overexpressing CMT-ARS mutants exhibit the same types of neuromuscular junction deficits seen in mouse models [37, 38].

MATERIALS AND METHODS

Cell culture, transfection, and neurite outgrowth assay

PC12, MN1, and HEK-293 cells were maintained under sterile conditions in a tissue culture incubator kept at 37˚ C and 5% CO_2. PC12 and MN1 cells were kind gifts from Rae Nishi and Anthony Antonellis, respectively. MN1 and HEK-293 cells were cultured in high-glucose DMEM (Corning, Tewksbury MA, USA) supplemented with 10% fetal bovine serum (Peak Serum, Wellington CO, USA), penicillin-streptomycin (Gibco, Gaithersburg, MD, USA), and L-glutamine (Gibco). PC12 cells were cultured in suspension using RPMI-1640 media (Corning) supplemented with 10% horse serum (Gibco), 5% fetal bovine serum, penicillin-streptomycin, and L-glutamine. Cells were adhered to a 6-well tissue culture plate coated with .25mg/mL poly D-lysine and then transfected with 5μg of plasmid DNA encoding wild-type or CMT-mutant HARS1 using lipofectamine 2000 (Invitrogen, Waltham MA, USA) diluted in OptiMEM (Gibco). The DNA/lipofectamine mixture was left on cells for six hours, after which full growth media was replaced and cells were allowed to recover overnight. Following transfection, PC12 cells were trypsinized and plated at low density on glass coverslips coated with 0.5 mg/mL poly D-lysine (Sigma, St. Louis MO, USA) and 0.02 mg/mL laminin. Differentiation was induced by treatment with 50 ng/μl β-NGF (Alamone, Jerusalem, Israel) in RPMI-1640 media supplemented with B27 (Thermo Scientific, Waltham MA, USA). Cells were allowed to differentiate for three days. Following differentiation cells were washed with cold PBS and fixed for 15 minutes at room temperature with 10% formalin. Neurites were labeled by staining with a GFP antibody (Abcam Ab290, Cambridge, UK) as described below. After coverslips were stained for GFP, they were mounted to glass slides and imaged on an epifluorescence microscope. A random number generator was used to select images for analysis, after which images were blinded, and the size of the cell body and neurites were measured using SPOT software. To ensure that non-differentiated cells were not accounted for – no data was obtained from cells without neurites, and cells with a longest neurite less than 10 microns were also not analyzed.

Immunofluorescence microscopy and image analysis

Cells to be analyzed by immunofluorescence microscopy were grown on coated glass coverslips and transfected and differentiated as described above. Following differentiation, cells were washed with PBS and fixed with 10% formalin for 15 minutes at room temperature. After fixation, blocking and permeabilization was performed by treating cells with 0.1% Triton® X-100 in 5% BSA-PBS. Coverslips were then stained overnight in a humidity chamber at 4˚C with primary antibodies against GFP (Abcam ab290) or p-eIF2α (Ser51, Abcam ab32157). Imaging was performed on either a Nikon Eclipse 50i epifluorescence microscope, or Nikon Eclipse Ti confocal microscope. After imaging of coverslips, a subset of images was selected using a random number generator and these images were blinded prior to analysis. Fluorescence intensity was determined by manually tracing cells using the GFP channel and measuring mean intensity of the channel of interest with ImageJ. Background fluorescence was measured and subtracted from intensity of the region of interest. For *in vivo* imaging, zebrafish were lightly anesthetized with tricaine hydrochloride and immobilized in 1.5% low melting point agarose dissolved in E3 buffer. A

small amount (200–300 μl) of E3 buffer was pipetted onto the agarose to provide nutritive support to the zebrafish during imaging. Using a Nikon Eclipse Ti confocal microscope, optical slices were obtained from above and below the PNS neurons being imaged and reconstructed using ImageJ. Images were blinded prior to analysis and axon length of the eight most anterior segments was measured using SPOT software. For analysis of DRG axon morphology, the first eight segments of each fish were analyzed, and axons were considered to be misguided when they overlapped with DRG axons at surrounding segments, or when they projected in a non-ventral direction and failed to reach their target.

OP-puromycin assay

To determine the rate of protein synthesis in differentiated PC12 cells, the O-propargyl-puromycin (OPP) click chemistry kit was used (Invitrogen). Differentiated PC12 cells were treated with 20 μM OPP for 30 minutes. Cells were washed with PBS, fixed with 10% formalin, and then permeabilized with 0.5% Triton® X-100 in PBS at room temperature. The click-chemistry reaction was performed as described in the product protocol, and cells were then mounted to glass coverslips using prolong gold (Invitrogen). Coverslips were imaged on a Nikon Eclipse Ti confocal microscope, and images were chosen for analysis using a random number generator. After images were blinded, cells were manually traced using the GFP channel and fluorescence intensity corresponding to OPP was measured using ImageJ. Treatment with 50 μg/mL of cycloheximide for thirty minutes was used as a negative control.

Western blotting

Prior to lysis, cells were washed twice on ice with cold PBS and then were scraped in m-cell lytic (Sigma) supplemented with protease inhibitor cocktail (Sigma), sodium pyrophosphate, and sodium orthovanadate. Lysates were then centrifuged at 15,000 rpm for 20 minutes at 4˚C to pellet cell debris. Protein concentration was determined using standard Bradford assay (BioRad, Hercules CA, USA). Fifteen micrograms of total cell lysate were electrophoresed on a 10% TRIS-polyacrylamide gel and subsequently transferred to a nitrocellulose membrane (BioRad) in methanol containing transfer buffer. Blocking was performed at room temperature for one hour with 5% BSA (VWR life science, Radnor PA, USA) and blots were incubated overnight with primary antibody at 4˚C. Primary antibodies against p-eIF2α (S51 Cell Signaling 9721S, Danvers MA, USA), total eIF2α (Cell Signaling 2103S), GFP (Abcam Ab290), β-actin (Proteintech 66009, Rosemont IL, USA), and GAP-43 (Abcam ab75810) were used at concentrations recommended by the supplier. Horseradish peroxidase conjugated secondary antibodies were diluted 1:5000 in 3% BSA and blots were incubated for 60–90 minutes at room temperature. Clarity western ECL substrate (BioRad) was used to visualize blots on an Amersham Imager 600. Densitometry was quantified using ImageJ. Representative western blots for GAP-43 (Fig. 1L), p-eIF2α (Fig. 2H) and total eIF2α (Fig. 1L and 2H) are from the same blot but are presented in different figures to enhance the flow of the manuscript.

Co-Immunoprecipitation

HEK-293 cells were co-transfected with 5 μg of plasmid DNA encoding FLAG and GFP-tagged HARS1 as described above. Two days post-transfection, cells were washed twice on

ice with cold PBS and lysed using RIPA buffer supplemented with protease inhibitor cocktail, sodium pyrophosphate, and sodium orthovanadate. Immunoprecipitation of FLAG-tagged constructs was performed by incubating 50 μg of lysate with anti-FLAG M2 magnetic beads (Sigma) as described in the product protocol. Proteins were eluted by addition of Laemmli buffer and boiling at 95˚C for 10 minutes after which the eluted protein was subjected to western blotting as described above.

Analytical Ultracentrifugation

Analytical ultracentrifugation experiments were performed and the data analyzed essentially as previously described [82] [28]. Briefly, purified enzymes (WT, R137Q) were dialyzed into a buffer containing 10mM potassium phosphate buffer, 50 mM KCl, and no reducing agents. Protein concentration was adjusted to 0.9 OD units at 230 nm (2.1 μM). Sedimentation velocity experiments were performed by the Center for Analytical Ultracentrifugation of Macromolecular Assemblies at the University of Texas Health Science Center at San Antonio, and conducted at 20˚C, 35 K rpm, in a Beckman Optima XLI analytical ultracentrifuge using an An60Ti rotor and standard 2-channel epon centerpieces. All data were analyzed with UltraScan [83] as described in [84], with final refinement by the parametrically constrained spectrum analysis [85] and Monte Carlo analysis [86].

Zebrafish husbandry

All procedures were approved by the University of Vermont Institutional Animal Care and Use Committee Protocol Number: 14–053 and the University of Vermont Institutional Biosafety Committee Protocol Number: 14–024. Embryos were raised under standard conditions and staged as previously described [87, 88]. Strains used include: Tg(ngn1:GFP) to label sensory neurons [51] and Tg(mnx1:mCherry) to label motor neurons (provided by Christine Beattie, Ohio State University).

mRNA synthesis and microinjection

A plasmid encoding FLAG-tagged human HARS1 (pCAGIG) was kindly provided by Robert Jinks, and a T7 promoter was incorporated by polymerase chain reaction. mRNA was synthesized using the T7 message machine kit (Invitrogen) and poly A tailing was performed using the Invitrogen poly-A tailing kit. mRNA was isolated by lithium chloride precipitation and resuspended in nuclease free water. Quantification was performed by the UVM AGCT core using the Qubit bioanalyzer. Following zebrafish mating, 300 pg of mRNA was injected into zebrafish at the 1–2 cell stage using an Eppendorf Femtojet 4i microinjector.

Zebrafish Touch Response Assay

Two days after fertilization and mRNA microinjection, fish were assigned to a numbered petri dish such that the experimenter was blinded to the treatment condition. After the fish acclimated to their new environment for five minutes, they were mechanically stimulated using forceps, with stimuli being applied at one to two second intervals. Swimming behavior was video recorded and then analyzed. The sensory component of the touch response was

analyzed by quantifying the percentage of touches that elicited a swim response, and motor responses were categorized as absent, abnormal, or normal. Swimming behavior was considered abnormal when fish fail to display typical sinusoidal swimming pattern.

Supplementary Material

Refer to Web version on PubMed Central for supplementary material.

ACKNOWLEDGEMENTS

We thank Rob Burgess and Ya-Ming Hou for discussions and feedback on the manuscript. Major support for the project was provided by NIGMS 5R01GM054899–20 (C.F.). B.D. acknowledges support from NIH (R01GM120600). Supercomputer calculations were performed at the Texas Advanced Computing Center and the San Diego Supercomputing Center supported through NSF/XSEDE grant TG-MCB070039N (B.D.). Graphical abstract was created using biorender.com.

Abbreviations

CMT	Charcot-Marie-Tooth disease
ARS	aminoacyl-tRNA synthetases
HARS1	cytoplasmic histidyl-tRNA synthetase
PC12	rat pheochromocytoma cells
GFP	green fluorescent protein
RFP	red fluorescent protein
eIF2α	eukaryotic initiation factor 2 subunit α
CMT2	axonal Charcot-Marie-Tooth disease
CMT1	demyelinating Charcot-Marie-Tooth disease
tRNA	transfer ribonucleic acid
GARS1	glycyl-tRNA synthetase
YARS1	cytoplasmic tyrosyl-tRNA synthetase
AARS1	cytoplasmic alanyl-tRNA synthetase
WARS1	cytoplasmic tryptophanyl-tRNA synthetase
NGF	nerve growth factor
GAP-43	growth associated protein-43
CHX	cycloheximide
PNS	peripheral nervous system
ngn1	neurogenin 1

mnx1	motor neuron and pancreas homeobox 1
DRG	dorsal root ganglion
hars	zebrafish histidyl-tRNA synthetase
hpf	hours post-fertilization
HisOH	histidinol
GCN2	general control nonderepressible 2
ISR	integrated stress response
PBS	phosphate buffered saline
CMT1B	Charcot-Marie-Tooth disease type 1B
CMT2B	Charcot-Marie-Tooth disease type 2B
HisRS	*E. coli* histidyl-tRNA synthetase
hts1	Yeast histidyl-tRNA synthetase
grs1	Yeast glycyl-tRNA synthetase

REFERENCES

1. Barreto LC, Oliveira FS, Nunes PS, de Franca Costa IM, Garcez CA, Goes GM, Neves EL, de Souza Siqueira Quintans J & de Souza Araujo AA (2016) Epidemiologic Study of Charcot-Marie-Tooth Disease: A Systematic Review, Neuroepidemiology. 46, 157–65. [PubMed: 26849231]
2. Pareyson D & Marchesi C (2009) Diagnosis, natural history, and management of Charcot-Marie-Tooth disease, Lancet Neurol. 8, 654–67. [PubMed: 19539237]
3. Skre H (1974) Genetic and clinical aspects of Charcot-Marie-Tooth's disease, Clin Genet. 6, 98–118. [PubMed: 4430158]
4. Baets J, De Jonghe P & Timmerman V (2014) Recent advances in Charcot-Marie-Tooth disease, Curr Opin Neurol. 27, 532–40. [PubMed: 25110935]
5. Berger P, Niemann A & Suter U (2006) Schwann cells and the pathogenesis of inherited motor and sensory neuropathies (Charcot-Marie-Tooth disease), Glia. 54, 243–57. [PubMed: 16856148]
6. Bussmann J & Storkebaum E (2017) Molecular pathogenesis of peripheral neuropathies: insights from Drosophila models, Curr Opin Genet Dev. 44, 61–73. [PubMed: 28213160]
7. Timmerman V, Strickland AV & Zuchner S (2014) Genetics of Charcot-Marie-Tooth (CMT) Disease within the Frame of the Human Genome Project Success, Genes. 5, 13–32. [PubMed: 24705285]
8. Meyer-Schuman R & Antonellis A (2017) Emerging Mechanisms of Aminoacyl-tRNA Synthetase Mutations in Recessive and Dominant Human Disease, Hum Mol Genet.
9. Wei N, Zhang Q & Yang XL (2019) Neurodegenerative Charcot-Marie-Tooth disease as a case study to decipher novel functions of aminoacyl-tRNA synthetases, J Biol Chem. 294, 5321–5339. [PubMed: 30643024]
10. Ibba M & Soll D (2001) The renaissance of aminoacyl-tRNA synthesis, EMBO Rep. 2, 382–7. [PubMed: 11375928]
11. Boczonadi V, Jennings MJ & Horvath R (2018) The role of tRNA synthetases in neurological and neuromuscular disorders, FEBS Lett. 592, 703–717. [PubMed: 29288497]
12. Cao X, Li C, Xiao S, Tang Y, Huang J, Zhao S, Li X, Li J, Zhang R & Yu W (2017) Acetylation promotes TyrRS nuclear translocation to prevent oxidative damage, Proc Natl Acad Sci U S A. 114, 687–692. [PubMed: 28069943]

13. Jeong SJ, Park S, Nguyen LT, Hwang J, Lee EY, Giong HK, Lee JS, Yoon I, Lee JH, Kim JH, Kim HK, Kim D, Yang WS, Kim SY, Lee CY, Yu K, Sonenberg N, Kim MH & Kim S (2019) A threonyl-tRNA synthetase-mediated translation initiation machinery, Nat Commun. 10, 1357. [PubMed: 30902983]

14. Williams TF, Mirando AC, Wilkinson B, Francklyn CS & Lounsbury KM (2013) Secreted Threonyl-tRNA synthetase stimulates endothelial cell migration and angiogenesis, Scientific Reports. 3, 1317. [PubMed: 23425968]

15. Yannay-Cohen N, Carmi-Levy I, Kay G, Yang CM, Han JM, Kemeny DM, Kim S, Nechushtan H & Razin E (2009) LysRS serves as a key signaling molecule in the immune response by regulating gene expression, Mol Cell. 34, 603–11. [PubMed: 19524539]

16. Fuchs SA, Schene IF, Kok G, Jansen JM, Nikkels PGJ, van Gassen KLI, Terheggen-Lagro SWJ, van der Crabben SN, Hoeks SE, Niers LEM, Wolf NI, de Vries MC, Koolen DA, Houwen RHJ, Mulder MF & van Hasselt PM (2019) Aminoacyl-tRNA synthetase deficiencies in search of common themes, Genet Med. 21, 319–330. [PubMed: 29875423]

17. Storkebaum E (2016) Peripheral neuropathy via mutant tRNA synthetases: Inhibition of protein translation provides a possible explanation, Bioessays. 38, 818–29. [PubMed: 27352040]

18. Griffin LB, Sakaguchi R, McGuigan D, Gonzalez MA, Searby C, Zuchner S, Hou YM & Antonellis A (2014) Impaired function is a common feature of neuropathy-associated glycyl-tRNA synthetase mutations, Hum Mutat. 35, 1363–71. [PubMed: 25168514]

19. Liao YC, Liu YT, Tsai PC, Chang CC, Huang YH, Soong BW & Lee YC (2015) Two Novel De Novo GARS Mutations Cause Early-Onset Axonal Charcot-Marie-Tooth Disease, PLoS One. 10, e0133423. [PubMed: 26244500]

20. Jordanova A, Irobi J, Thomas FP, Van Dijck P, Meerschaert K, Dewil M, Dierick I, Jacobs A, De Vriendt E, Guergueltcheva V, Rao CV, Tournev I, Gondim FA, D'Hooghe M, Van Gerwen V, Callaerts P, Van Den Bosch L, Timmermans JP, Robberecht W, Gettemans J, Thevelein JM, De Jonghe P, Kremensky I & Timmerman V (2006) Disrupted function and axonal distribution of mutant tyrosyl-tRNA synthetase in dominant intermediate Charcot-Marie-Tooth neuropathy, Nat Genet. 38, 197–202. [PubMed: 16429158]

21. Hyun YS, Park HJ, Heo SH, Yoon BR, Nam SH, Kim SB, Park CI, Choi BO & Chung KW (2014) Rare variants in methionyl- and tyrosyl-tRNA synthetase genes in late-onset autosomal dominant Charcot-Marie-Tooth neuropathy, Clin Genet. 86, 592–4. [PubMed: 24354524]

22. Latour P, Thauvin-Robinet C, Baudelet-Mery C, Soichot P, Cusin V, Faivre L, Locatelli MC, Mayencon M, Sarcey A, Broussolle E, Camu W, David A & Rousson R (2010) A major determinant for binding and aminoacylation of tRNA(Ala) in cytoplasmic Alanyl-tRNA synthetase is mutated in dominant axonal Charcot-Marie-Tooth disease, Am J Hum Genet. 86, 77–82. [PubMed: 20045102]

23. McLaughlin HM, Sakaguchi R, Giblin W, Program NCS, Wilson TE, Biesecker L, Lupski JR, Talbot K, Vance JM, Zuchner S, Lee YC, Kennerson M, Hou YM, Nicholson G & Antonellis A (2012) A recurrent loss-of-function alanyl-tRNA synthetase (AARS) mutation in patients with Charcot-Marie-Tooth disease type 2N (CMT2N), Hum Mutat. 33, 244–53. [PubMed: 22009580]

24. Zhao Z, Hashiguchi A, Hu J, Sakiyama Y, Okamoto Y, Tokunaga S, Zhu L, Shen H & Takashima H (2012) Alanyl-tRNA synthetase mutation in a family with dominant distal hereditary motor neuropathy, Neurology. 78, 1644–9. [PubMed: 22573628]

25. Weterman MAJ, Kuo M, Kenter SB, Gordillo S, Karjosukarso DW, Takase R, Bronk M, Oprescu S, van Ruissen F, Witteveen RJW, Bienfait HME, Breuning M, Verhamme C, Hou YM, de Visser M, Antonellis A & Baas F (2018) Hypermorphic and hypomorphic AARS alleles in patients with CMT2N expand clinical and molecular heterogeneities, Hum Mol Genet. 27, 4036–4050. [PubMed: 30124830]

26. Vester A, Velez-Ruiz G, McLaughlin HM, Program NCS, Lupski JR, Talbot K, Vance JM, Zuchner S, Roda RH, Fischbeck KH, Biesecker LG, Nicholson G, Beg AA & Antonellis A (2013) A loss-of-function variant in the human histidyl-tRNA synthetase (HARS) gene is neurotoxic in vivo, Hum Mutat. 34, 191–9. [PubMed: 22930593]

27. Safka Brozkova D, Deconinck T, Griffin LB, Ferbert A, Haberlova J, Mazanec R, Lassuthova P, Roth C, Pilunthanakul T, Rautenstrauss B, Janecke AR, Zavadakova P, Chrast R, Rivolta C, Zuchner S, Antonellis A, Beg AA, De Jonghe P, Senderek J, Seeman P & Baets J (2015) Loss of

function mutations in HARS cause a spectrum of inherited peripheral neuropathies, Brain. 138, 2161–72. [PubMed: 26072516]

28. Abbott JA, Meyer-Schuman R, Lupo V, Feely S, Mademan I, Oprescu SN, Griffin LB, Alberti MA, Casasnovas C, Aharoni S, Basel-Vanagaite L, Zuchner S, De Jonghe P, Baets J, Shy ME, Espinos C, Demeler B, Antonellis A & Francklyn C (2018) Substrate interaction defects in histidyl-tRNA synthetase linked to dominant axonal peripheral neuropathy, Hum Mutat. 39, 415–432. [PubMed: 29235198]
29. Tsai PC, Soong BW, Mademan I, Huang YH, Liu CR, Hsiao CT, Wu HT, Liu TT, Liu YT, Tseng YT, Lin KP, Yang UC, Chung KW, Choi BO, Nicholson GA, Kennerson ML, Chan CC, De Jonghe P, Cheng TH, Liao YC, Zuchner S, Baets J & Lee YC (2017) A recurrent WARS mutation is a novel cause of autosomal dominant distal hereditary motor neuropathy, Brain.
30. Stum M, McLaughlin HM, Kleinbrink EL, Miers KE, Ackerman SL, Seburn KL, Antonellis A & Burgess RW (2011) An assessment of mechanisms underlying peripheral axonal degeneration caused by aminoacyl-tRNA synthetase mutations, Mol Cell Neurosci. 46, 432–43. [PubMed: 21115117]
31. Froelich CA & First EA (2011) Dominant Intermediate Charcot-Marie-Tooth disorder is not due to a catalytic defect in tyrosyl-tRNA synthetase, Biochemistry. 50, 7132–45. [PubMed: 21732632]
32. Antonellis A, Lee-Lin SQ, Wasterlain A, Leo P, Quezado M, Goldfarb LG, Myung K, Burgess S, Fischbeck KH & Green ED (2006) Functional analyses of glycyl-tRNA synthetase mutations suggest a key role for tRNA-charging enzymes in peripheral axons, Journal of Neuroscience. 26, 10397–406. [PubMed: 17035524]
33. Xie W, Nangle LA, Zhang W, Schimmel P & Yang XL (2007) Long-range structural effects of a Charcot-Marie-Tooth disease-causing mutation in human glycyl-tRNA synthetase, Proc Natl Acad Sci U S A. 104, 9976–81. [PubMed: 17545306]
34. Nangle LA, Zhang W, Xie W, Yang XL & Schimmel P (2007) Charcot-Marie-Tooth disease-associated mutant tRNA synthetases linked to altered dimer interface and neurite distribution defect, Proc Natl Acad Sci U S A. 104, 11239–44. [PubMed: 17595294]
35. Malissovas N, Griffin LB, Antonellis A & Beis D (2016) Dimerization is required for GARS-mediated neurotoxicity in dominant CMT disease, Hum Mol Genet. 25, 1528–42. [PubMed: 27008886]
36. Niehues S, Bussmann J, Steffes G, Erdmann I, Kohrer C, Sun L, Wagner M, Schafer K, Wang G, Koerdt SN, Stum M, Jaiswal S, RajBhandary UL, Thomas U, Aberle H, Burgess RW, Yang XL, Dieterich D & Storkebaum E (2015) Impaired protein translation in Drosophila models for Charcot-Marie-Tooth neuropathy caused by mutant tRNA synthetases, Nat Commun. 6, 7520. [PubMed: 26138142]
37. Seburn KL, Nangle LA, Cox GA, Schimmel P & Burgess RW (2006) An active dominant mutation of glycyl-tRNA synthetase causes neuropathy in a Charcot-Marie-Tooth 2D mouse model, Neuron. 51, 715–26. [PubMed: 16982418]
38. Spaulding EL, Sleigh JN, Morelli KH, Pinter MJ, Burgess RW & Seburn KL (2016) Synaptic Deficits at Neuromuscular Junctions in Two Mouse Models of Charcot-Marie-Tooth Type 2d, J Neurosci. 36, 3254–67. [PubMed: 26985035]
39. Sleigh JN, Grice SJ, Burgess RW, Talbot K & Cader MZ (2014) Neuromuscular junction maturation defects precede impaired lower motor neuron connectivity in Charcot-Marie-Tooth type 2D mice, Hum Mol Genet.
40. He W, Bai G, Zhou H, Wei N, White NM, Lauer J, Liu H, Shi Y, Dumitru CD, Lettieri K, Shubayev V, Jordanova A, Guergueltcheva V, Griffin PR, Burgess RW, Pfaff SL & Yang XL (2015) CMT2D neuropathy is linked to the neomorphic binding activity of glycyl-tRNA synthetase, Nature. 526, 710–4. [PubMed: 26503042]
41. Royer-Bertrand B, Tsouni P, Mullen P, Campos Xavier B, Mittaz Crettol L, Lobrinus AJ, Ghika J, Baumgartner MR, Rivolta C, Superti-Furga A, Kuntzer T, Francklyn C & Tran C (2019) Peripheral neuropathy and cognitive impairment associated with a novel monoallelic HARS variant, Ann Clin Transl Neurol. 6, 1072–1080. [PubMed: 31211171]
42. Bond S, Lopez-Lloreda C, Gannon PJ, Akay-Espinoza C & Jordan-Sciutto KL (2020) The Integrated Stress Response and Phosphorylated Eukaryotic Initiation Factor 2alpha in Neurodegeneration, J Neuropathol Exp Neurol. 79, 123–143. [PubMed: 31913484]

43. Tatsumi Y, Matsumoto N, Iibe N, Watanabe N, Torii T, Sango K, Homma K, Miyamoto Y, Sakagami H & Yamauchi J (2019) CMT type 2N disease-associated AARS mutant inhibits neurite growth that can be reversed by valproic acid, Neurosci Res. 139, 69–78. [PubMed: 30261202]
44. Das KP, Freudenrich TM & Mundy WR (2004) Assessment of PC12 cell differentiation and neurite growth: a comparison of morphological and neurochemical measures, Neurotoxicol Teratol. 26, 397–406. [PubMed: 15113601]
45. Cogli L, Progida C, Lecci R, Bramato R, Kruttgen A & Bucci C (2010) CMT2B-associated Rab7 mutants inhibit neurite outgrowth, Acta Neuropathol. 120, 491–501. [PubMed: 20464402]
46. Vester A, Velez-Ruiz G, McLaughlin HM, Lupski JR, Talbot K, Vance JM, Zuchner S, Roda RH, Fischbeck KH, Biesecker LG, Nicholson G, Beg AA & Antonellis A (2013) A loss-of-function variant in the human histidyl-tRNA synthetase (HARS) gene is neurotoxic in vivo, Hum Mutat. 34, 191–9. [PubMed: 22930593]
47. Arnez JG, Augustine JG, Moras D & Francklyn CS (1997) The first step of aminoacylation at the atomic level in histidyl-tRNA synthetase, Proc Natl Acad Sci, USA. 94, 7144–9. [PubMed: 9207058]
48. Vaughan MH & Hansen BS (1973) Control of initiation of protein synthesis in human cells. Evidence for a role of uncharged transfer ribonucleic acid, J Biol Chem. 248, 7087–96. [PubMed: 4743514]
49. Harding HP, Ordonez A, Allen F, Parts L, Inglis AJ, Williams RL & Ron D (2019) The ribosomal P-stalk couples amino acid starvation to GCN2 activation in mammalian cells, Elife. 8.
50. Newman EM, Nierenberg DW & Santi DV (1983) Selective killing of transformed cells by methotrexate with histidine deprivation or with alpha-amino alcohols, Cancer Res. 43, 4703–8. [PubMed: 6883328]
51. Blader P, Plessy C & Strahle U (2003) Multiple regulatory elements with spatially and temporally distinct activities control neurogenin1 expression in primary neurons of the zebrafish embryo, Mech Dev. 120, 211–8. [PubMed: 12559493]
52. Zelenchuk TA & Bruses JL (2011) In vivo labeling of zebrafish motor neurons using an mnx1 enhancer and Gal4/UAS, Genesis. 49, 546–54. [PubMed: 21538811]
53. Wallen RC & Antonellis A (2013) To charge or not to charge: mechanistic insights into neuropathy-associated tRNA synthetase mutations, Curr Opin Genet Dev. 23, 302–9. [PubMed: 23465884]
54. Zhang X, Ling J, Barcia G, Jing L, Wu J, Barry BJ, Mochida GH, Hill RS, Weimer JM, Stein Q, Poduri A, Partlow JN, Ville D, Dulac O, Yu TW, Lam AT, Servattalab S, Rodriguez J, Boddaert N, Munnich A, Colleaux L, Zon LI, Soll D, Walsh CA & Nabbout R (2014) Mutations in QARS, encoding glutaminyl-tRNA synthetase, cause progressive microcephaly, cerebral-cerebellar atrophy, and intractable seizures, Am J Hum Genet. 94, 547–58. [PubMed: 24656866]
55. Siekierska A, Stamberger H, Deconinck T, Oprescu SN, Partoens M, Zhang Y, Sourbron J, Adriaenssens E, Mullen P, Wiencek P, Hardies K, Lee JS, Giong HK, Distelmaier F, Elpeleg O, Helbig KL, Hersh J, Isikay S, Jordan E, Karaca E, Kecskes A, Lupski JR, Kovacs-Nagy R, May P, Narayanan V, Pendziwiat M, Ramsey K, Rangasamy S, Shinde DN, Spiegel R, Timmerman V, von Spiczak S, Helbig I, Group CRR, Consortium, A. R. w. g. o. t. E. R., Weckhuysen S, Francklyn C, Antonellis A, de Witte P & De Jonghe P (2019) Biallelic VARS variants cause developmental encephalopathy with microcephaly that is recapitulated in vars knockout zebrafish, Nat Commun. 10, 708. [PubMed: 30755616]
56. Antonellis A, Oprescu SN, Griffin LB, Heider A, Amalfitano A & Innis JW (2018) Compound heterozygosity for loss-of-function FARSB variants in a patient with classic features of recessive aminoacyl-tRNA synthetase-related disease, Hum Mutat. 39, 834–840. [PubMed: 29573043]
57. Friedman J, Smith DE, Issa MY, Stanley V, Wang R, Mendes MI, Wright MS, Wigby K, Hildreth A, Crawford JR, Koehler AE, Chowdhury S, Nahas S, Zhai L, Xu Z, Lo WS, James KN, Musaev D, Accogli A, Guerrero K, Tran LT, Omar TEI, Ben-Omran T, Dimmock D, Kingsmore SF, Salomons GS, Zaki MS, Bernard G & Gleeson JG (2019) Biallelic mutations in valyl-tRNA synthetase gene VARS are associated with a progressive neurodevelopmental epileptic encephalopathy, Nat Commun. 10, 707. [PubMed: 30755602]
58. Kuo ME & Antonellis A (2019) Ubiquitously Expressed Proteins and Restricted Phenotypes: Exploring Cell-Specific Sensitivities to Impaired tRNA Charging, Trends Genet.

59. He W, Zhang HM, Chong YE, Guo M, Marshall AG & Yang XL (2011) Dispersed disease-causing neomorphic mutations on a single protein promote the same localized conformational opening, Proc Natl Acad Sci U S A. 108, 12307–12. [PubMed: 21737751]
60. Blocquel D, Li S, Wei N, Daub H, Sajish M, Erfurth ML, Kooi G, Zhou J, Bai G, Schimmel P, Jordanova A & Yang XL (2017) Alternative stable conformation capable of protein misinteraction links tRNA synthetase to peripheral neuropathy, Nucleic Acids Res. 45, 8091–8104. [PubMed: 28531329]
61. Blocquel D, Sun L, Matuszek Z, Li S, Weber T, Kuhle B, Kooi G, Wei N, Baets J, Pan T, Schimmel P & Yang XL (2019) CMT disease severity correlates with mutation-induced open conformation of histidyl-tRNA synthetase, not aminoacylation loss, in patient cells, Proc Natl Acad Sci U S A. 116, 19440–19448. [PubMed: 31501329]
62. Sleigh JN, Dawes JM, West SJ, Wei N, Spaulding EL, Gomez-Martin A, Zhang Q, Burgess RW, Cader MZ, Talbot K, Yang XL, Bennett DL & Schiavo G (2017) Trk receptor signaling and sensory neuron fate are perturbed in human neuropathy caused by Gars mutations, Proc Natl Acad Sci U S A. 114, E3324–E3333. [PubMed: 28351971]
63. Mo Z, Zhao X, Liu H, Hu Q, Chen XQ, Pham J, Wei N, Liu Z, Zhou J, Burgess RW, Pfaff SL, Caskey CT, Wu C, Bai G & Yang XL (2018) Aberrant GlyRS-HDAC6 interaction linked to axonal transport deficits in Charcot-Marie-Tooth neuropathy, Nat Commun. 9, 1007. [PubMed: 29520015]
64. Benoy V, Van Helleputte L, Prior R, d'Ydewalle C, Haeck W, Geens N, Scheveneels W, Schevenels B, Cader MZ, Talbot K, Kozikowski AP, Vanden Berghe P, Van Damme P, Robberecht W & Van Den Bosch L (2018) HDAC6 is a therapeutic target in mutant GARS-induced Charcot-Marie-Tooth disease, Brain. 141, 673–687. [PubMed: 29415205]
65. Adams RA, Fernandes-Cerqueira C, Notarnicola A, Mertsching E, Xu Z, Lo WS, Ogilvie K, Chiang KP, Ampudia J, Rosengren S, Cubitt A, King DJ, Mendlein JD, Yang XL, Nangle LA, Lundberg IE, Jakobsson PJ & Schimmel P (2019) Serum-circulating His-tRNA synthetase inhibits organ-targeted immune responses, Cell Mol Immunol.
66. Morelli KH, Griffin LB, Pyne NK, Wallace LM, Fowler AM, Oprescu SN, Takase R, Wei N, Meyer-Schuman R, Mellacheruvu D, Kitzman JO, Kocen SG, Hines TJ, Spaulding EL, Lupski JR, Nesvizhskii A, Mancias P, Butler IJ, Yang XL, Hou YM, Antonellis A, Harper SQ & Burgess RW (2019) Allele-specific RNA interference prevents neuropathy in Charcot-Marie-Tooth disease type 2D mouse models, J Clin Invest. 129, 5568–5583. [PubMed: 31557132]
67. Oprescu SN, Griffin LB, Beg AA & Antonellis A (2017) Predicting the pathogenicity of aminoacyl-tRNA synthetase mutations, Methods. 113, 139–151. [PubMed: 27876679]
68. Chihara T, Luginbuhl D & Luo L (2007) Cytoplasmic and mitochondrial protein translation in axonal and dendritic terminal arborization, Nat Neurosci. 10, 828–37. [PubMed: 17529987]
69. Kuo ME & Antonellis A (2020) Ubiquitously Expressed Proteins and Restricted Phenotypes: Exploring Cell-Specific Sensitivities to Impaired tRNA Charging, Trends Genet. 36, 105–117. [PubMed: 31839378]
70. Lek M, Karczewski KJ, Minikel EV, Samocha KE, Banks E, Fennell T, O'Donnell-Luria AH, Ware JS, Hill AJ, Cummings BB, Tukiainen T, Birnbaum DP, Kosmicki JA, Duncan LE, Estrada K, Zhao F, Zou J, Pierce-Hoffman E, Berghout J, Cooper DN, Deflaux N, DePristo M, Do R, Flannick J, Fromer M, Gauthier L, Goldstein J, Gupta N, Howrigan D, Kiezun A, Kurki MI, Moonshine AL, Natarajan P, Orozco L, Peloso GM, Poplin R, Rivas MA, Ruano-Rubio V, Rose SA, Ruderfer DM, Shakir K, Stenson PD, Stevens C, Thomas BP, Tiao G, Tusie-Luna MT, Weisburd B, Won HH, Yu D, Altshuler DM, Ardissino D, Boehnke M, Danesh J, Donnelly S, Elosua R, Florez JC, Gabriel SB, Getz G, Glatt SJ, Hultman CM, Kathiresan S, Laakso M, McCarroll S, McCarthy MI, McGovern D, McPherson R, Neale BM, Palotie A, Purcell SM, Saleheen D, Scharf JM, Sklar P, Sullivan PF, Tuomilehto J, Tsuang MT, Watkins HC, Wilson JG, Daly MJ, MacArthur DG & Exome Aggregation C (2016) Analysis of protein-coding genetic variation in 60,706 humans, Nature. 536, 285–91. [PubMed: 27535533]
71. Guth E, Farris M, Bovee M & Francklyn CS (2009) Asymmetric amino acid activation by class II histidyl-tRNA synthetase from Escherichia coli, J Biol Chem. 284, 20753–62. [PubMed: 19487703]

72. Guth EC & Francklyn CS (2007) Kinetic discrimination of tRNA identity by the conserved motif 2 loop of a class II aminoacyl-tRNA synthetase, Molecular Cell. 25, 531–42. [PubMed: 17317626]
73. Hansen BS, Vaughan MH & Wang L (1972) Reversible inhibition by histidinol of protein synthesis in human cells at the activation of histidine, J Biol Chem. 247, 3854–7. [PubMed: 4338230]
74. Darnell AM, Subramaniam AR & O'Shea EK (2018) Translational Control through Differential Ribosome Pausing during Amino Acid Limitation in Mammalian Cells, Mol Cell. 71, 229–243 e11. [PubMed: 30029003]
75. Inglis AJ, Masson GR, Shao S, Perisic O, McLaughlin SH, Hegde RS & Williams RL (2019) Activation of GCN2 by the ribosomal P-stalk, Proc Natl Acad Sci U S A. 116, 4946–4954. [PubMed: 30804176]
76. Schneider-Poetsch T, Ju J, Eyler DE, Dang Y, Bhat S, Merrick WC, Green R, Shen B & Liu JO (2010) Inhibition of eukaryotic translation elongation by cycloheximide and lactimidomycin, Nat Chem Biol. 6, 209–217. [PubMed: 20118940]
77. Storkebaum E, Leitao-Goncalves R, Godenschwege T, Nangle L, Mejia M, Bosmans I, Ooms T, Jacobs A, Van Dijck P, Yang XL, Schimmel P, Norga K, Timmerman V, Callaerts P & Jordanova A (2009) Dominant mutations in the tyrosyl-tRNA synthetase gene recapitulate in Drosophila features of human Charcot-Marie-Tooth neuropathy, Proc Natl Acad Sci U S A. 106, 11782–7. [PubMed: 19561293]
78. Achilli F, Bros-Facer V, Williams HP, Banks GT, AlQatari M, Chia R, Tucci V, Groves M, Nickols CD, Seburn KL, Kendall R, Cader MZ, Talbot K, van Minnen J, Burgess RW, Brandner S, Martin JE, Koltzenburg M, Greensmith L, Nolan PM & Fisher EM (2009) An ENU-induced mutation in mouse glycyl-tRNA synthetase (GARS) causes peripheral sensory and motor phenotypes creating a model of Charcot-Marie-Tooth type 2D peripheral neuropathy, Dis Model Mech. 2, 359–73. [PubMed: 19470612]
79. Waldron AL, Cahan SH, Francklyn CS & Ebert AM (2017) A single Danio rerio hars gen encodes both cytoplasmic and mitochondrial Histidyl-tRNA Synthetases, PLOS ONE. 12(9), e018531.
80. Babin PJ, Goizet C & Raldua D (2014) Zebrafish models of human motor neuron diseases: advantages and limitations, Prog Neurobiol. 118, 36–58. [PubMed: 24705136]
81. Wang M, Wen H & Brehm P (2008) Function of neuromuscular synapses in the zebrafish choline-acetyltransferase mutant bajan, J Neurophysiol. 100, 1995–2004. [PubMed: 18684905]
82. Abbott JA, Guth E, Kim C, Regan C, Siu VM, Rupar CA, Demeler B, Francklyn CS & Robey-Bond SM (2017) The Usher Syndrome Type IIIB Histidyl-tRNA Synthetase Mutation Confers Temperature Sensitivity, Biochemistry. 56, 3619–3631. [PubMed: 28632987]
83. Demeler B & Gorbet GE (2016) Analytical Ultracentrifugation Data Analysis with UltraScan-III in In Analytical Ultracentrifugation: Instrumentation, Software, and Applications (Uchiyama S, Arisaka F, Stafford WF & Laue T, eds) pp. 119–143, Springer, Tokyo.
84. Demeler B (2010) Methods for the design and analysis of sedimentation velocity and sedimentation equilibrium experiments with proteins, Curr Protoc Protein Sci Chapter 7, Unit 7 13.
85. Gorbet G, Devlin T, Hernandez Uribe BI, Demeler AK, Lindsey ZL, Ganji S, Breton S, Weise-Cross L, Lafer EM, Brookes EH & Demeler B (2014) A parametrically constrained optimization method for fitting sedimentation velocity experiments, Biophys J. 106, 1741–50. [PubMed: 24739173]
86. Demeler B, and Brookes E (2008) Monte Carlo analysis of sedimentation experiments, Colloid and Polymer Science. 286, 129–137.
87. Kimmel CB, Ballard WW, Kimmel SR, Ullmann B & Schilling TF (1995) Stages of embryonic development of the zebrafish, Dev Dyn. 203, 253–310. [PubMed: 8589427]
88. Westerfield M (2000) The Zebrafish Book: A Guide for the Laboratory Use of Zebrafish (Danio Rerio) 4th edn, University of Oregon Press, Eugene, OR.

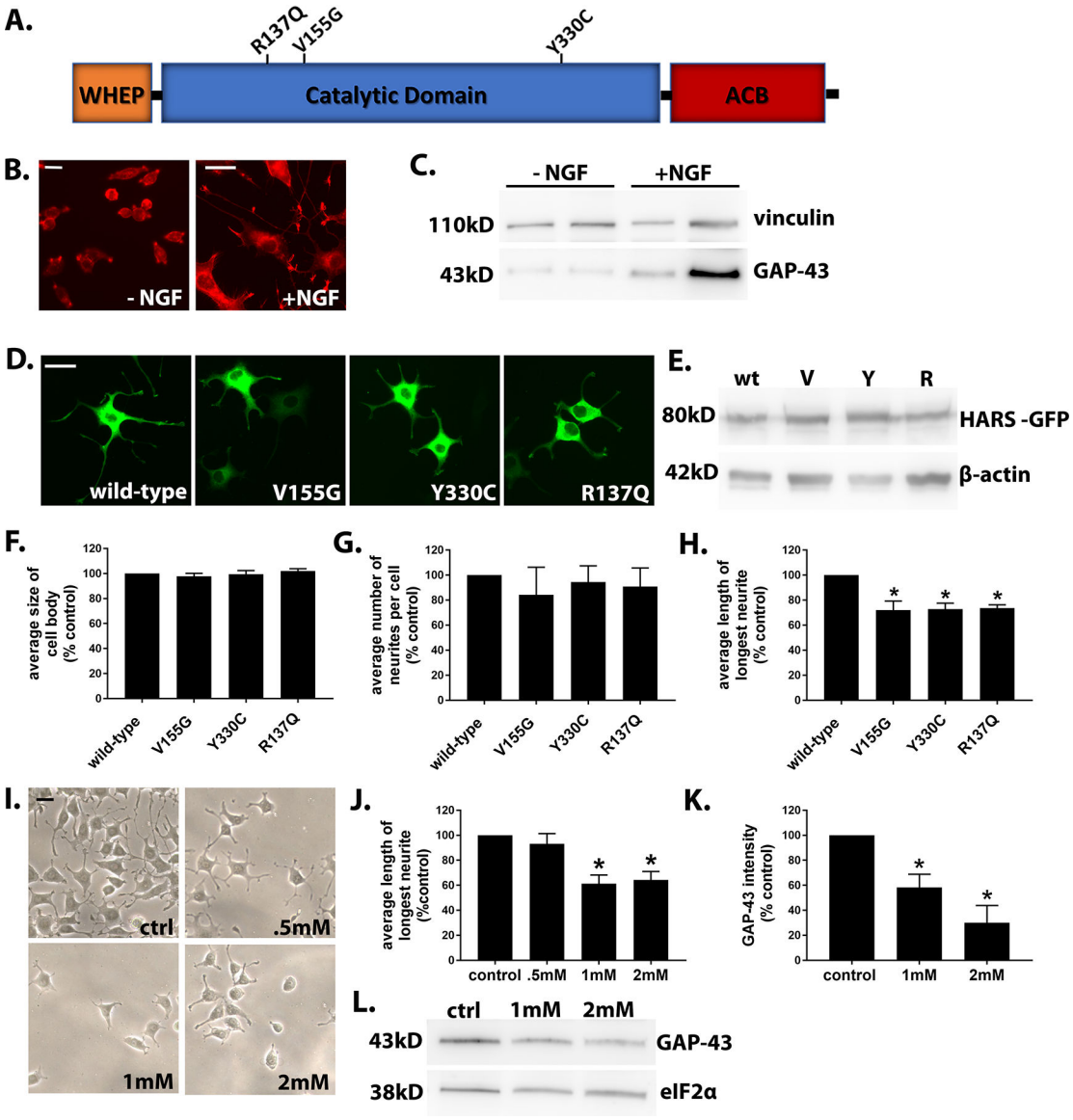

Figure 1.

Expression of CMT-HARS1 and treatment with histidinol impairs NGF-induced neurite outgrowth in PC12 cells. (A) Schematic representation of human HARS1 with the location of CMT-HARS1 mutations indicated. (B) Application of 50 ng/mL β-NGF to the culture media of PC12 cells results in the elaboration of neurite processes, cells were stained with phalloidin-594. (C) Lysates from NGF treated PC12 cells were analyzed by immunoblotting for the differentiation marker GAP-43 and loading control, vinculin. (D) PC12 cells transfected with plasmids encoding GFP tagged HARS1 were differentiated with β-NGF, stained for GFP and imaged. (E) Lysates from transfected and differentiated PC12 cells were analyzed for levels of wild-type and CMT-HARS1 by immunoblotting for GFP. (F-H) PC12 cells transfected with either wild-type or CMT-HARS1 expression plasmids were differentiated and SPOT software was used to measure cell body size (F), number of neurites per cell (G), and length of longest neurite (H). (I,J) Brightfield images of differentiated PC12

cells treated with 0–2 mM histidinol and measurement of the length of longest neurite (J). (K,L) Lysates from β-NGF stimulated PC12 cells treated with 0–2 mM histidinol were analyzed for GAP-43 levels by immunoblotting. Data represents mean +/− SEM from three separate experiments, * indicates significant difference from wild-type or control ($p<.05$) by one-way ANOVA. For neurite outgrowth assays, n=3 averages from separate experiments. Western blot n=3 blots with lysate from separate passages. Scale bar = 20μm.

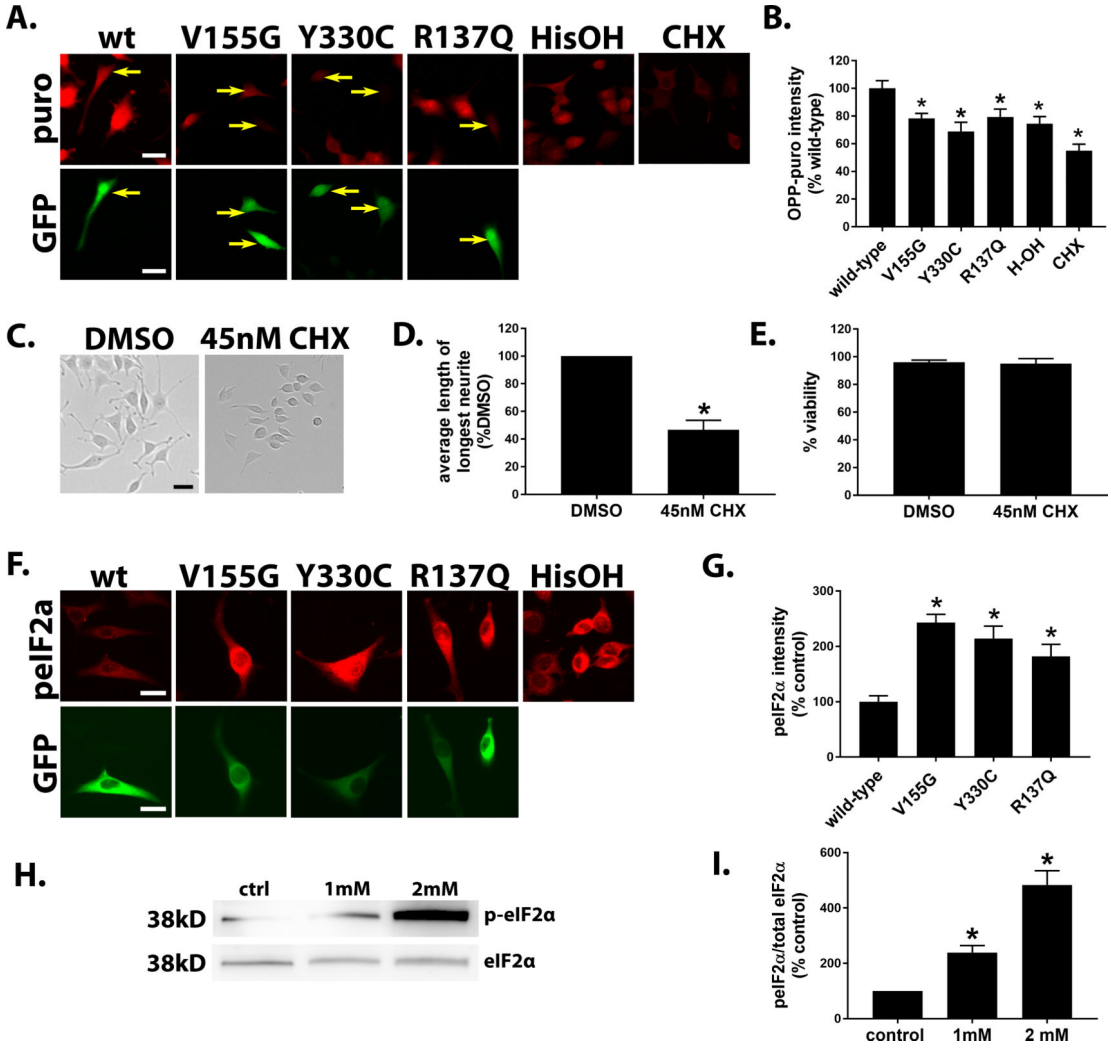

Figure 2.

Expression of CMT-HARS1 attenuates protein synthesis and increases phosphorylation of eIF2α in differentiated PC12 cells. (A) Transfected and differentiated PC12 cells were treated with OP-puromycin and Alexa-594 was attached to puromycin by ‘click-chemistry’ reaction. (B) Quantitation of Alexa-594 intensity in differentiated PC12 cells expressing CMT-HARS. (C-E) Neurite outgrowth assay in PC12 cells treated with cycloheximide (CHX) and quantitation of cell viability by trypan blue staining (E). (F,G) Immunostaining for phosphorylated eIF2α (F) and measurement of fluorescence intensity (G) in differentiated PC12 cells expressing CMT-HARS1. (H,I) Western blot analysis of eIF2α phosphorylation in differentiated PC12 cells treated with 0–2 mM histidinol. Data represents mean +/− SEM from three separate experiments. * indicates significant difference compared to wild-type or control ($p < .05$) by one-way ANOVA or two-tailed unpaired t-test, respectively. For click-chemistry experiment, wild-type n=69 cells, V155G n=98, Y330C n=45, R137Q n=58, histidinol n=55, cycloheximide n=61. For p-eIF2α immunofluorescence imaging, wild-type n=42 cells, V155G n=50, Y330C n=44, R137Q n=31. Neurite outgrowth

assay n=3 averages from separate experiments. Viability was measured at three separate passages. Western blot n=3 blots with lysate from separate passages. Scale bar = 20 μm.

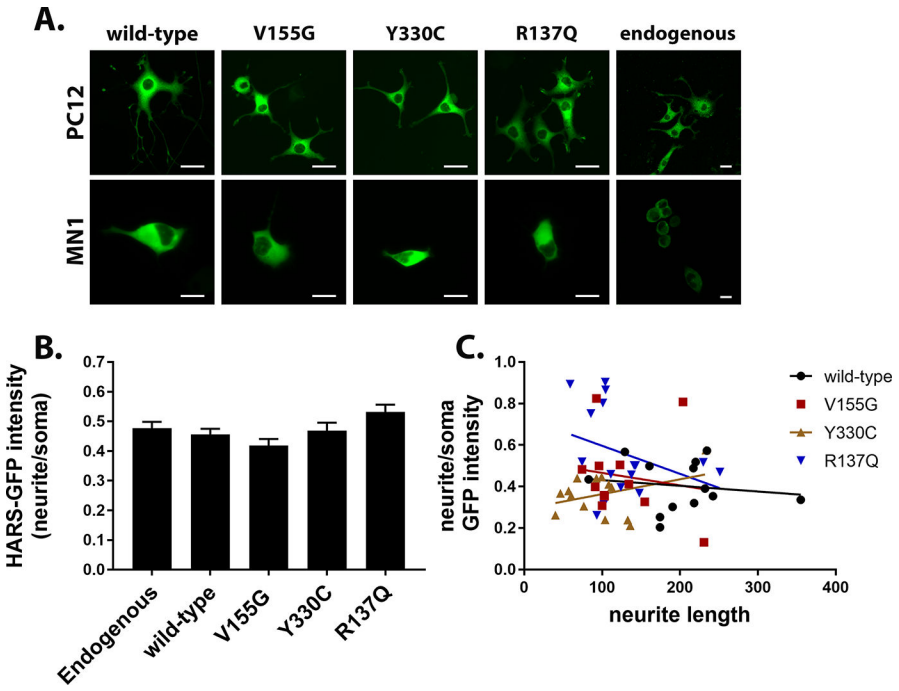

Figure 3.

Mutant HARS1 proteins localize normally in PC12 and MN1 cells. (A) PC12 (upper row) and MN1 (lower row) cells were transfected with GFP-tagged HARS1 and stained for GFP to analyze localization of mutant protein compared to wild-type. (B) Ratio of HARS1 fluorescence intensity in the nerite to cell body of PC12 cells is consistent between wild-type transfected, mutant transfected, and endogenous HARS1. (C) Correlation of intensity of HARS1 staining in neurites with neurite length in differentiated PC12 cells. Data represents mean +/− SEM from two independent experiments. B, wild-type n=43 neurites, V155G n=50, Y330C n=52, R137Q n=42, endogenous n=55.C, n=55 neurites. Scale bar = 20 μm.

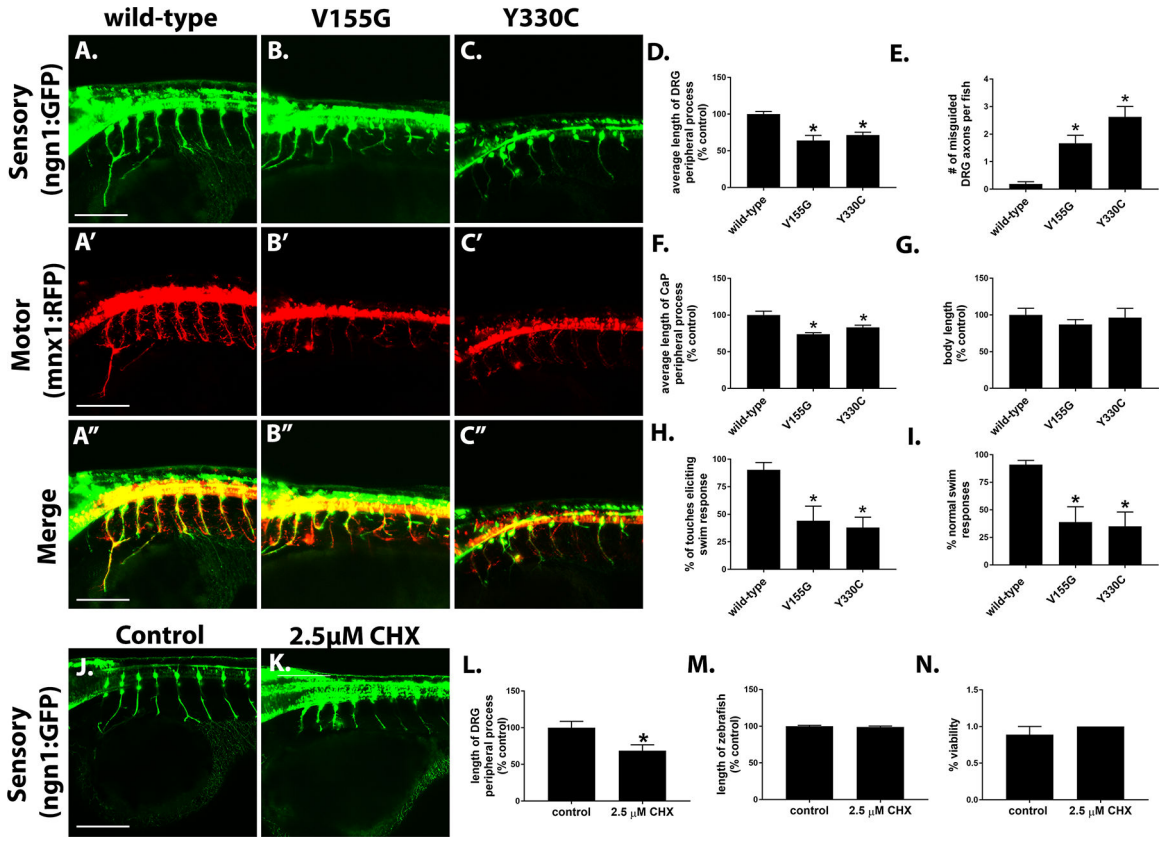

Figure 4.

Expression of Y330C and V155G HARS1 disrupts structure and function of the peripheral nervous system in vivo. (A-C') mRNA encoding human wild-type or mutant HARS1 was microinjected at the one-cell stage into transgenic zebrafish embryos expressing fluorescent proteins under the control of promoters specific to sensory (ngn1:GFP) (A-C) and motor (mnx1:RFP) (A'-C') neurons of the peripheral nervous system. (D-F) Developing animals were imaged live at 48 hpf and axon length (D,F) and patterning (E) was analyzed following reconstruction of confocal z-stacks. (G) Brightfield imaging was used for measurement of zebrafish body length. (H,I) Touch response assay was used to analyze responsiveness to touch stimuli (H) and swimming behavior (I). (J-N) Measurement of DRG length (J-L), body length (M), and viability (N) in zebrafish treated with 2.5 μM CHX at 24 hpf. Data is shown as mean +/− SEM from three independent experiments. * indicates significant difference from wild-type or control ($p < .05$) by one-way ANOVA or two-tailed unpaired t-test, respectively. Wild-type n=18 animals, V155G n=18, Y330C n=21. Control n=10 animals, cycloheximide n=14. Viability was measured in three separate clutches of embryos. Scale bar = 100 μm.

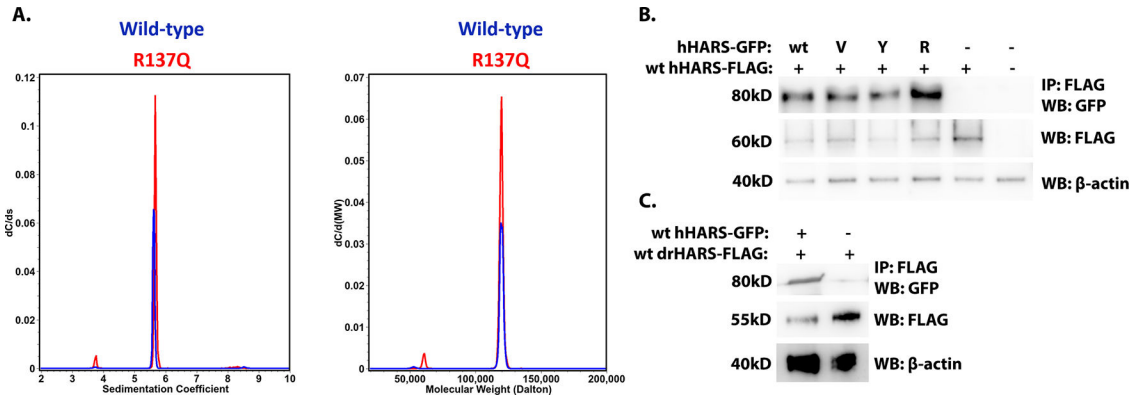

Figure 5.

CMT mutant HARS1 proteins form heterodimers with wild-type HARS1 in HEK-293 cells. (A) Analytical sedimentation coefficient and molar mass distributions for wild-type (blue) and R137Q (red) HARS1 confirming homogeneous samples and dimer state for both proteins. (B) Immunoprecipitation of FLAG-tagged wild-type HARS1 and immunoblotting for GFP-tagged wild-type or mutant HARS1 to identify the presence of wild-type-mutant heterodimers in transfected HEK cells. (C) Immunoprecipitation of FLAG-tagged wild-type zebrafish hars (drHARS) and immunoblotting for GFP-tagged human HARS1 (hHARS1) to identify hHARS1 drHARS heterodimers in transfected HEK cells. Immunoprecipitation experiments (B,C) were repeated twice (n=2).